Near edge x-ray absorption fine structure measurements of the interface between bottom antireflective coatings and a model deprotected photoresist

Erin L. Jablonski,[a] Sharadha Sambasivan, and Eric K. Lin
Polymers Division, National Institute of Standards and Technology, Gaithersburg, Maryland 20899

Daniel A. Fischer
Ceramics Division, National Institute of Standards and Technology, Gaithersburg, Maryland 20899

Chelladurai Devadoss and Rama Puligadda
Brewer Science, Inc., Rolla, Missouri 65401

(Received 24 June 2003; accepted 2 September 2003; published 10 December 2003)

The interface between bottom anti-reflective coatings (BARCs) and a model deprotected photoresist, poly(4-hydroxystyrene) (PHS), was investigated using near edge x-ray absorption fine structure spectroscopy to identify mechanisms responsible for pattern degradation at the BARC/photoresist interface. Interactions at this interface can lead to pattern deviations such as footing, undercut, and pattern collapse. It was found that a residual layer is only formed when the bilayer is subject to ultraviolet exposure. The spectra of the BARC surfaces after photoresist processing and development show a combination of spectral features from both PHS and the BARC formulations. The data suggest that the residual layer results from interactions between crosslinker and photoresist that occur during normal photoresist processing. © *2003 American Vacuum Society.* [DOI: 10.1116/1.1621661]

I. INTRODUCTION

Bottom antireflective coatings (BARCs) are used in optical microlithography between the silicon substrate and photoresist film to minimize standing waves, provide thin film interference effects (at the appropriate thickness), and prevent reflective notching from substrate reflections during ultraviolet (UV) exposure. In this way, BARCs provide better resolution and critical dimension control.[1,2] As feature sizes are reduced, the exposure wavelength of microlithography tools decreases; with decreasing exposure wavelength the optical interference effects due to substrate reflection become more severe as the reflectivity of the silicon substrate in general increases with decreasing wavelength. Hence, the use of BARCs in integrated circuit manufacture becomes more important with decreasing feature size (wavelength).

Though BARCs play a beneficial role in microlithography by minimizing optical interference effects, in some cases they are also a source of unwanted problems by interacting or intermixing with the photoresist layer. It is desirable to obtain orthogonal, undistorted photoresist profiles after developing; however, the chemically amplified photoresists that are currently used in deep UV (i.e., 248 and 193 nm exposure) lithography are prone to interfacial interactions which lead to deviations in the photoresist profile such as footing, undercut, and pattern collapse.[3–5] The model organic BARCs considered here are cross-linked polymer networks; the formulations comprise BARC resin (polymer and photoabsorbing dye), a crosslinking agent, and an acid component that catalyzes the crosslinking reaction during the curing process. In a typical photoresist formulation, there is photoresist polymer and, among other small molecule additives, a photo-acid generator that decomposes to produce acid during UV exposure to catalyze the deprotection reaction responsible for the solubility switch in positive-tone chemically amplified photoresists. Since the deprotection reaction is sensitive to acid concentration, surface interactions between the BARC acid component and photogenerated acid and other BARC and photoresist components are a potential cause of pattern deviations. Despite suppressing interdiffusion and small molecule migration to a large extent by crosslinking the BARC film, interactions between BARC and photoresist still occur. It is essential to minimize the adverse interactions between the BARC and photoresist to obtain undistorted resist profiles while maintaining sufficient adhesion between the BARC and photoresist layer so that the patterns do not collapse.

The objective of this study is to characterize the chemical nature of BARC/photoresist interfacial interactions to provide guidance for the design and formulation of organic BARCs. To address this issue, the surface chemical properties of BARC and residual layer (the layer of deprotected photoresist remaining on the surface of the BARC film after development) films were characterized using near edge x-ray absorption fine structure (NEXAFS) spectroscopy.[6] The composition of the residual layer was studied as a function of BARC formulation.

II. EXPERIMENT

A. Materials and methods

A commercially available BARC formulation (Brewer Science, Inc.) and variations having excess (double) or low

[a]Electronic mail: erin.jablonski@nist.gov

 1071-1023/2003/21(6)/3153/4/$19.00 ©2003 American Vacuum Society

(half) quantity of crosslinker or acid catalyst were used with neat poly(4-hydroxystyrene) (PHS). A silicon wafer was spin coated with each BARC formulation and cured at 205 °C for 60 s. For residual layers, PHS was spin coated from a PGMEA solution over a cured BARC layer and subsequent processing steps were carried out. Half were processed with the same postapply bake (PAB) (130 °C, 60 s), UV exposure from a broadband source ($15\ mJ/cm^2$), postexposure bake (PEB) (130 °C, 60 s), and development. The others underwent PAB and PEB, but were not UV exposed.

B. NEXAFS

NEXAFS measurements were conducted at the U7A beam line of the National Synchrotron Light Source at Brookhaven National Laboratory. The experimental conditions have been described elsewhere.[6] The spectra were collected with the incident beam at the magic angle (54.7°) relative to the sample to remove any polarization dependence. For the NEXAFS spectra in this article the experimental standard uncertainty in the peak position is $\approx \pm 0.15$ eV. The relative uncertainty in the NEXAFS intensity is less than $\pm 5\%$ and was determined by multiple scans on a sample.

In a typical NEXAFS experiment, soft x rays are preferentially absorbed by the sample when the incident radiation is at the appropriate energy to allow the excitation of a core shell electron to an unoccupied molecular orbital. Due to the well-defined energy gap associated with a core shell to unoccupied orbital transition, NEXAFS is sensitive to the bonding characteristics of the atom giving a discrete peak for each chemical bonding environment. Auger electrons are emitted when the excited core electron from the irradiated sample relaxes. The electrons emitted deep within the film cannot escape; only the electrons emitted near the top (1–6 nm for carbon *K*-edge electron yield spectra) of the film surface have enough kinetic energy to escape the surface potential. The electron yield detector has a grid where a negative voltage bias can be applied. The electrons that escape the surface of the film but are emitted from furthest within the film are low in energy due to inelastic interactions with other atoms. These low energy electrons may not have enough kinetic energy to pass the negative detector bias and are not detected. If the negative detector bias voltage is gradually increased, progressively higher kinetic energy electrons are detected, and the effective electron yield sampling depth gets closer to the film surface.

III. RESULTS AND DISCUSSION

The NEXAFS carbon *K*-edge electron yield spectra of the BARC without additives, some of the BARC formulations used in this study (cured only), and PHS are shown in Fig. 1: (a) BARC resin, no catalyst or crosslinker; (b) low crosslinker, regular catalyst; (c) regular formulation; (d) excess crosslinker, regular catalyst; and (e) PHS, at different bias voltages. All spectra are pre- and postedge jump normalized. Postedge normalization eliminates the spectral dependence on total carbon content; therefore, changes in the

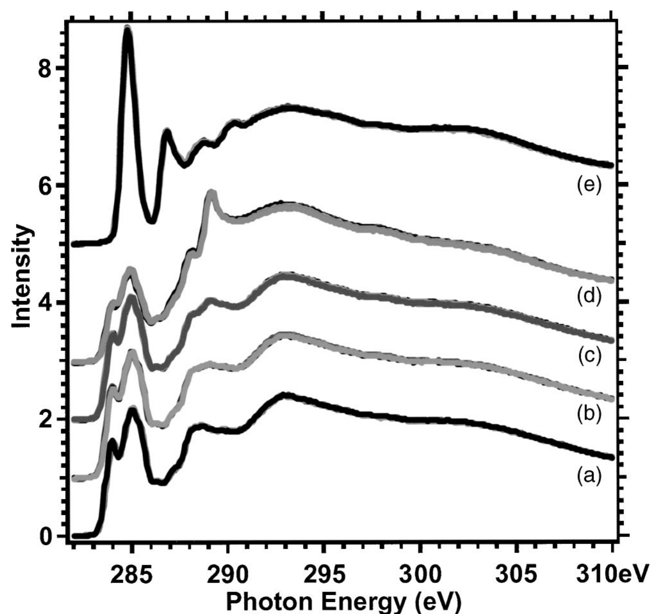

FIG. 1. NEXAFS carbon *K*-edge electron yield spectra at variable detector bias: (a) BARC resin; (b) low crosslinker; (c) regular formulation; (d) excess crosslinker; and (e) PHS. Spectra are vertically offset for clarity.

NEXAFS spectra are indicative of changes in the chemical functionality. The spectra of the formulations having excess and low catalyst are not shown because there are no distinguishable spectral features compared to the regular formulation. In each of (a)–(e), spectra taken at −50, −100, −150, and −200 V bias are overlaid. Comparison of the spectra at the different bias voltages shows that the chemical composition of the cured BARC surface does not change from 2 nm (−200 V bias) to 6 nm (−50 V bias) into the film. The spectra shown in Fig. 1 will provide the component spectra of the linear combination fits for the residual layer spectra shown below.

In Fig. 1(a), the peak at 284.0 eV corresponds to the $C\,1s \rightarrow \pi^*_{C=C}$ transition from the phenyl groups of the photoabsorbing dye.[7] The next prominent peak, at 285.0 eV, is the $C\,1s \rightarrow \pi^*_{C=C}$ transition from the phenyl groups of the photoabsorbing dye as well as phenyl groups of the polymer. The small peak at 286.3 eV represents a splitting of the $C\,1s \rightarrow \pi^*_{C=C}$ transition. The very distinct peak in Fig. 1(d) at 289.1 eV is attributable to the $C\,1s \rightarrow \pi^*_{C=O}$ transition from the crosslinker molecule. This peak is smaller in the 1(b) formulation containing low the typical crosslinker concentration, and completely absent in 1(a), containing no crosslinker.

Figure 2 shows the carbon *K*-edge electron yield spectra of the BARC surface after development of the unexposed PHS films at −50 and −200 V. There is no residual PHS layer. However, the surface of the BARC has changed. Due to increased crosslinker and decreased acid catalyst (possibly washed away by developer), the spectra of the BARCs after having a PHS film removed from them did not match those of the original BARC surface, with the exception of the excess crosslinker formulation. Rather, the processed BARC

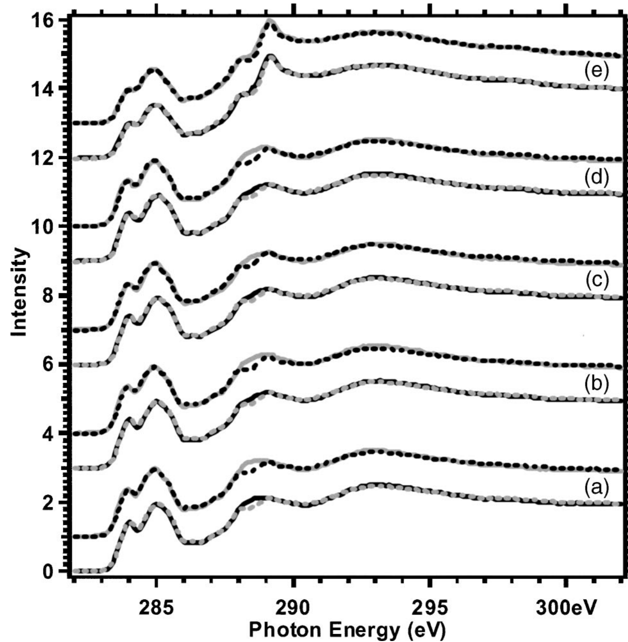

FIG. 2. NEXAFS carbon K-edge electron yield spectra of unexposed BARC surface after PHS development at −50 and −200 V detector bias: (a) low crosslinker; (b) low catalyst; (c) regular formulation; (d) excess catalyst; and (e) excess crosslinker. Solid lines are experimental data, dashed lines represent linear combination fits to the spectra, as shown in Table I. Spectra are vertically offset for clarity.

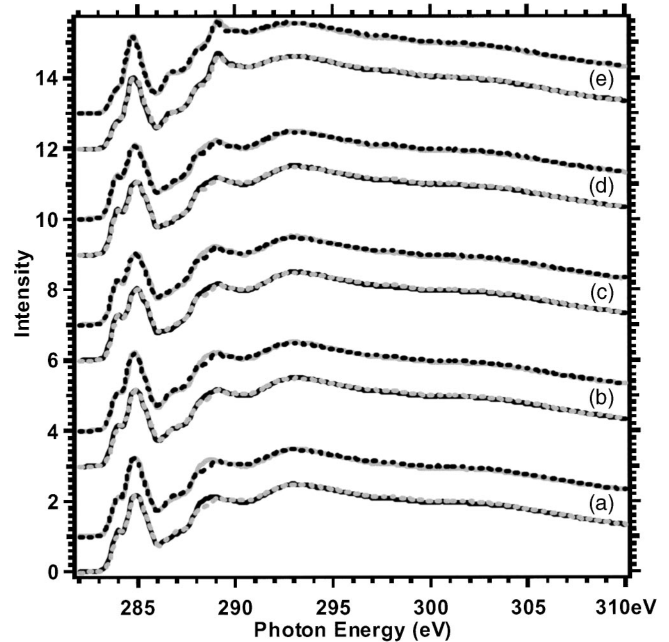

FIG. 3. NEXAFS carbon K-edge electron yield spectra of UV exposed PHS/BARC residual layers at −50 and −200 V detector bias: (a) low crosslinker; (b) low catalyst; (c) regular formulation; (d) excess catalyst; and (e) excess crosslinker. Solid lines are experimental data, dashed lines represent linear combination fits to the spectra, as shown in Table II. Spectra are vertically offset for clarity.

surfaces were best represented by a combination of the BARC resin spectra and the excess crosslinker spectra, as shown in Table I. There is also the appearance of a low energy carbonyl peak (region 287.5–289 eV), the source of which cannot be identified at this time but is suspected to be a result of interactions with the developer solution. The excess crosslinker spectra are overlaid with the original spectra of the cured-only BARC formulation having excess crosslinker.

In Fig. 2, solid curves are the experimental spectra and dashed curves represent a linear combination of the component (BARC resin and excess crosslinker) spectra at the corresponding voltage bias. For example, as shown in Table I, the −50 V bias spectra of developed PHS on the regular formulation BARC is best fit by a combination of 65% BARC resin spectra [Fig. 1(a)] and 35% excess crosslinker spectra [Fig. 1(d)]. For comparison, the original regular formulation spectra was found to be fit well by 20% excess crosslinker spectra, 80% BARC resin, and the original low crosslinker spectra was fit by 10% excess crosslinker spectra and 90% BARC resin (fits not shown).

TABLE I. Compositions of the linear combinations of component spectra used to fit the spectra of various PHS processed BARC formulations. The error of these fits is ≈±5%.

BARC component of residual layer	Voltage bias (V)	Component NEXAFS spectra	
		Excess crosslinker	BARC resin
Regular	−50	0.35	0.65
	−200	0.40	0.60
Low crosslinker	−50	0.30	0.70
	−200	0.34	0.66
Excess catalyst	−50	0.38	0.62
	−200	0.43	0.57
Low catalyst	−50	0.35	0.65
	−200	0.38	0.62

If the PHS/BARC bilayers were exposed to UV, the resulting surface was quite different. After exposure, a significant amount of PHS remained on the BARC and the residual layer was up to ≈30% photoresist component for the residual layer on BARC with excess crosslinker. This result suggests the crosslinker is undergoing an unknown reaction and effectively "sticking" the PHS to the surface. While the specific reaction has not yet been elucidated, other studies have found that reduced crosslinker concentration in the BARC formulation reduces residual layer formation.[8] The crosslinker may also act as a dissolution inhibitor, preventing complete dissolution of PHS.

The NEXAFS carbon K-edge electron yield spectra of various UV exposed residual layers of PHS on the BARC formulations are shown in Fig. 3: (a) low crosslinker, regular catalyst; (b) low catalyst, regular crosslinker; (c) regular formulation; (d) excess catalyst, regular crosslinker; and (e) excess crosslinker, regular catalyst; all at −50 and −200 V biases. The experimental spectra are shown by the solid curves, fits are shown by dashed curves, and details are given in Table II. The regular formulation BARC gave the lowest

TABLE II. Compositions of the linear combinations of component spectra used to fit the spectra of residual layers of PHS on various BARC formulations.

BARC component of residual layer	Voltage bias (V)	Component NEXAFS spectra		
		Excess cross linker	BARC resin	PHS
Regular	−50	0.32	0.60	0.08
	−200	0.36	0.57	0.07
Excess crosslinker	−50	0.75	0.00	0.25
	−200	0.67	0.00	0.33
Low crosslinker	−50	0.25	0.53	0.22
	−200	0.28	0.50	0.22
Excess catalyst	−50	0.33	0.55	0.12
	−200	0.34	0.54	0.12
Low catalyst	−50	0.30	0.50	0.20
	−200	0.33	0.45	0.22

PHS component of the residual layer. The formulations having low crosslinker and low catalyst both gave ≈20% PHS component in the residual layer; it is possible that the BARC surface was incompletely crosslinked, allowing diffusion of PHS.

Although the residual layer on the excess catalyst formulation had less PHS component, excess catalyst on the BARC surface could cause adhesion and/or dissolution problems during normal photoresist processing.[9]

IV. CONCLUSIONS

The chemical composition of residual layers of PHS on various BARC formulations was measured with NEXAFS. Irrespective of possible BARC components' interference with the photoresist deprotection reaction, it was found that PHS, a model deprotected photoresist, forms a residual layer on the BARC surface after UV exposure. This shows that interactions between the BARC and photoresist layers occur during normal photoresist processing steps (PAB, UV exposure, PEB) and that footing may occur at the BARC/photoresist interface as a result of interactions between photoresist and crosslinking agent.

ACKNOWLEDGMENTS

The authors thank the Missile Defense Agency (MDA) for financial support through Phase II Program Contract No. DASG60-1-C0047. E.L.J. acknowledges support by an NRC-NIST post-doctoral fellowship. Runhui Huang assisted with sample preparation and characterization. Certain commercial equipment, instruments, or materials are identified in this article in order to specify the experimental procedure adequately. Such identification is not intended to imply recommendation or endorsement by the National Institute of Standards and Technology, nor is it intended to imply that the materials or equipment are necessarily the best available for this purpose.

[1]J. E. Lamb III, Semiconductor Fabtech **2**, 223 (1995).
[2]J. Sturtevant and B. Roman, Microlithogr. World 13 (1995).
[3]H. Yoshino, T. Itani, S. Hashimoto, M. Yamana, T. Yashii, and H. Tanabe, Proc. SPIE **3333**, 655 (1998).
[4]H. B. Cao, P. F. Nealey, and W.-D. Domke, J. Vac. Sci. Technol. B **18**, 3303 (2000).
[5]J. Simons, D. L. Goldfarb, M. Angelopoulos, S. Messick, W. Moreau, C. Robinson, J. De Pablo, and P. Nealey, Proc. SPIE **4345**, 19 (2001).
[6]J. L. Lenhart, R. L. Jones, E. K. Lin, C. L. Soles, W.-I. Wu, D. A. Fischer, S. Sambasivan, D. L. Goldfarb, and M. Angelopoulos, J. Vac. Sci. Technol. B **20**, 2920 (2002).
[7]H. Oji, R. Mitsumoto, E. Ito, H. Ishii, Y. Ouchi, K. Seki, T. Yokoyama, T. Ohta, and N. Kosugi, J. Chem. Phys. **109**, 10409 (1998).
[8]B. De, S. Malik, S. Dilocker, G. Spaziano, J. Biafore, and M. Bowden, J. Macromol. Sci., Pure Appl. Chem. **A39**, 1 (2002).
[9]C. Devadoss, Y. Wang, R. Puligadda, J. L. Lenhart, E. L. Jablonski, D. A. Fischer, S. Sambasivan, E. K. Lin, and W.-l. Wu, Proc. SPIE (submitted 2003).